

Study of the Intermediate Mass Ratio Black Hole Binary Merger up to 1000:1 with Numerical Relativity

Carlos O. Lousto and James Healy
Center for Computational Relativity and Gravitation (CCRG),
School of Mathematical Sciences, Rochester Institute of Technology,
85 Lomb Memorial Drive, Rochester, New York 14623

(Dated: March 28, 2023)

We explicitly demonstrate that current numerical relativity techniques are able to accurately evolve black hole binaries with mass ratios of the order of 1000:1. This proof of principle is relevant for future third generation (3G) gravitational wave detectors and space mission LISA, as by purely numerical methods we would be able to accurately compute gravitational waves from the last stages of black hole mergers, as directly predicted by general relativity. We perform a sequence of simulations in the intermediate to small mass ratio regime, $m_1^p/m_2^p = 1/7, 1/16, 1/32, 1/64, 1/128, 1/256, 1/512, 1/1024$, with the small hole starting from rest at a proper distance $D \approx 13M$. We compare these headon full numerical evolutions with the corresponding semianalytic point particle perturbative results finding an impressive agreement for the total gravitational radiated energy and linear momentum as well as for the waveform spectra. We display numerical convergence of the results and identify the minimal numerical resolutions required to accurately solve for these very low amplitude gravitational waves. This work represents a first step towards the considerable challenge of applying numerical-relativity waveforms to interpreting gravitational-wave observations by LISA and next-generation ground-based gravitational-wave detectors.

INTRODUCTION

There is currently great interest in the binary black hole small mass ratio regime. On one hand, the direct detection of gravitational waves from binary black holes since GW150914[1] and the currently 90 new detections[2] by LIGO-Virgo show consistency with the detailed waveforms predictions of Numerical Relativity[3, 4] for comparable mass ratio binaries. Purely full numerical banks of waveforms [5] have been proven to be able and very effective for estimating binary black hole mergers parameters and directly applied to the (10+3) gravitational waves signals detected in the O1/O2 LIGO-Virgo observational runs [6].

On the other hand, the steady progress towards the establishment of a LISA launch and operation in the next decade [7], and the development of third generation (3G) ground detectors [8–10], highlights the necessity to expand the theoretical studies to much smaller mass ratios than are currently in use, most of them valid in the comparable mass-ratio-regime[6]. Scenarios involving intermediate mass black holes merging with supermassive black holes in the center of galaxies are targets for LISA [11] and stellar mass black holes merging with intermediate mass black hole are targets of 3G detectors, also leading small mass ratios mergers.

While different astrophysical scenarios may consider all sort of binary black hole systems, for the sake of definiteness, here we will refer to *comparable* mass ratios, $q = m_1/m_2$, as those in the range $0.1 < q \leq 1$, *intermediate* in the range $0.01 < q \leq 0.1$, *small* in the range $0.001 < q \leq 0.01$, and below that in the *near*, $10^{-5} < q \leq 10^{-3}$, *middle*, $10^{-7} < q \leq 10^{-5}$, and *far*,

$10^{-9} < q \leq 10^{-7}$, *extreme* mass ratio regimes. Most of the numerical simulations focus on the comparable masses cases, and perturbation theory realm is in that of the extreme mass ratios. In this work we display techniques that bridge this gap, performing binary black hole simulations in the intermediate to small mass ratio binaries regime.

The theoretical interest in the extreme mass ratio (particle limit) binaries precedes LIGO and LISA conceptions. The pioneering work of Regge and Wheeler [12] and Zerilli [13] laid down the formalism for first order perturbations around a single Schwarzschild black hole, and later work by Teukolsky[14] considered the more general Kerr black hole background. The consistency of this approach at higher perturbative orders, including not only radiation reaction but self-force on the smaller hole (particle), was proven much later by Mino, Sasaki, and Tanaka[15] and then by Quinn and Wald[16]. This approach proved hard to implement explicitly, but steady progress has been made since the early headon collisions[17, 18] to the current generic orbits (See Ref. [19] for a current status review).

Numerical Relativity remains the primary method on the forefront of computing gravitational waves and its results can be used to fit EOB, Phenom, Surrogate phenomenological models [20–22]. One of the important challenges for numerical relativity is the introduction of any new physical scale to be resolved accurately and, even if mesh refinement methods are applied, this remains in general computationally demanding. A first prototypical study of a 100:1 mass-ratio binary black hole in [23] produced the last two orbits before merger. The headon collision case was then numerically studied

in [24] (and its D -dimensional generalization in [25]). In [26] it was studied a binary black hole numerical simulation with spins and a mass ratio 18:1 and in [27] a 15:1 mass ratio case. A recent revisit to the small mass ratio problem [28] produced 13 orbits before merger for a 128:1 mass-ratio binary with moderate computational resources, leading then to the possibility of improving effective one body models in the small mass ratio regime [29] and covering the 3G detectors mass-ratios regime and LISA most conspicuous sources.

Still, LISA could be sensitive to even smaller mass ratio binaries, two orders of magnitude smaller, deep into the small mass-ratio regime [11]. This raises the question if Numerical Relativity can still provide accurate predictions for the waveforms, trajectories, and final remnant of the merger of such small mass ratio binary black holes. In this paper we explore the current limits of the methods of Numerical Relativity, in particular the moving punctures approach [3]. We will test our formalism in the regime of up to 1000:1 mass-ratio binaries. For this first prototypical study we will consider headon collisions from rest and compare them to the particle limit results (without the need to include self-force or radiation reaction computations). Our main goal here is to establish if the moving punctures method can resolve such extremely small levels of gravitational radiation (even lower amplitudes than in the orbital case) and if the results show convergence with increasing numerical resolution towards the corresponding expected (perturbative) values. This, in turn, can provide landmarks to reproduce as tests or to use in fits by semianalytic/phenomenological models [29].

NUMERICAL TECHNIQUES

In Ref. [28] we have studied the late inspiral and merger of small mass ratio binary black holes, reaching a 128:1 case performing 13 orbits before merger with the use of $\mathcal{O}(10)$ computational nodes. In order to perform this simulation we have used the LazEv code [30] with 8th order spatial finite differences [31], 4th order Runge-Kutta time integration with a Courant factor ($dt/dx = 1/4$). Crucially, we used a grid structure developed for the $q = 1/15$ simulations in [32] and adapted for the 128:1 with three additional refinement levels (15 total) from the boundaries of the simulation down to the horizon of the smaller hole.

We have performed several convergence and error studies of our numerical formalism. In Appendix A of Ref. [33], in Appendix B of Ref. [34], and in Ref. [35], we performed convergence studies for different mass ratios and spins of the binaries. In Ref. [4] and Ref. [36] we compared the RIT waveforms with those produced completely independently by the SXS collaboration finding excellent agreement, convergence towards each others results and matching of individual modes up to $l = 5$. In

Refs. [28, 37] we studied convergence for an orbiting binary with $q = 1/15$ for 10 orbits prior to merger as well as consistency between radiated and horizon quantities for up to $q = 1/128$ orbiting black hole binaries, and validation versus EOB models [29]. In [38] we have studied the accuracy of our simulations versus the Courant factor and concluded that while we can use $1/2$ for short runs, we can ensure long term evolutions with $1/4$, and not much gain was obtained by further reducing it to $1/8$. For LIGO-Virgo applications, we have found that $1/3$ was good enough for most of the simulations [5, 39–41].

In the present work we will include several important variations. We design a sequence of small mass ratio headon collisions from rest with decreasing mass ratios by factors of 2 and correspondingly add a new refinement level of half grid size tight around the small hole, in the Zeno's approach of [28] and keeping the deepest refinement level just above the small hole horizon. A second important difference here is in the use of the numerical gauge. In Ref. [37] we have found that the η parameter in the shift β^a (Gamma-driver) evolution equation

$$\partial_t \beta^a = \frac{3}{4} \tilde{\Gamma}^a - \eta(\vec{r}, t) \beta^a, \quad (1)$$

plays an important role in the accuracy of the results and the optimal use of the grid points to resolve the binary black hole dynamics and its gravitational radiation. In particular, the use of the $\eta(W)$ driven by the function of the evolved conformal factor $W = e^{-2\Phi}$ in [28] was seen to lead to numerical noise that can be avoided with the spatial coordinate \vec{r} dependent $\eta_G(\vec{r})$ choice, while preserving the properties of adapting to the spacetime around each such dispersed black hole sizes

$$\eta_G = \frac{\mathcal{A}}{m} + \frac{\mathcal{B}}{m_1} \left(\frac{\vec{r}_1(t)^2}{\vec{r}_1(t)^2 + \sigma_1^2} \right)^n e^{-|\vec{r} - \vec{r}_1(t)|^2 / \sigma_1^2} + \frac{\mathcal{C}}{m_2} \left(\frac{\vec{r}_2(t)^2}{\vec{r}_2(t)^2 + \sigma_2^2} \right)^n e^{-|\vec{r} - \vec{r}_2(t)|^2 / \sigma_2^2}, \quad (2)$$

with $\mathcal{A} = 1$, $\mathcal{B} = 1$, $\mathcal{C} = 1$; $\sigma_1 = 2m_1$, $\sigma_2 = 2m_2$, $n = 2$ used here. $\vec{r}_i(t)$ being the location of the punctures and m_i being the horizon masses of the holes, with $m = m_1 + m_2$.

In order to test the accuracy of our simulations against the results of first order perturbation theory, and to study its numerical convergence, we perform a first prototypical study of the direct plunge of a small black hole onto a large Schwarzschild black hole from rest at a reference isotropic coordinate $R_0 = 10M$, corresponding to a proper distance from the large hole horizon of $D/M = \int_{0.5}^{10} (1 + 1/2x)^2 dx = 12.9707$ (Here M is the total ADM mass of the system).

This choice allows us to study the merger of the holes using quadrant symmetry by placing the small black hole along the z -axis and hence reduce the numerical grid to one quarter of its full coverage. The grid structure of

TABLE I. Initial data parameters for the headon configurations with a smaller mass black hole (labeled as 1), and a larger mass spinning black hole (labeled as 2). The punctures are located at $\vec{r}_1 = (0, 0, z_1)$ and $\vec{r}_2 = (0, 0, z_2)$, have an initial simple proper distance [44] of D , with momenta $P_i = (0, 0, 0)$ and spin $S_i = (0, 0, 0)$, mass parameters m_i^p/M , total ADM mass $M_{\text{ADM}} = 1.0$, the configurations are denoted by qX, where $X = m_2^p/m_1^p$, while in the last column $q = m_1/m_2$ is in terms of the horizon masses.

Run	z_1/M	z_2/M	D/M	m_1^p/M	m_2^p/M	q
q7	-8.7500	1.2500	13.42	0.1250	0.8750	0.148181
q16	-9.4118	0.5882	13.26	0.0588	0.9412	0.065249
q32	-9.6970	0.3030	13.18	0.0303	0.9697	0.032716
q64	-9.8462	0.1538	13.13	0.0154	0.9846	0.016382
q128	-9.9225	0.0775	13.10	0.0078	0.9922	0.008197
q256	-9.9611	0.0389	13.09	0.0039	0.9961	0.004100
q512	-9.9805	0.0195	13.08	0.0019	0.9981	0.002050
q1024	-9.9902	0.0098	13.08	0.0010	0.9990	0.001025

our mesh refinements have a size of the largest box for all simulations of $\pm 400M$. The number of points between 0 and 400 on the coarsest grid is XXX in nXXX (i.e. n100 has 100 points). So, the grid spacing on the coarsest is $400/\text{XXX}$. The resolution in the wavezone is $100M/\text{XXX}$ (i.e. n100 has $M/1.00$, n206 has $M/2.06$). The grid around the larger black hole (m_2) is fixed at $\pm 1.0M$ in size and is the 9th refinement level. Therefore the grid spacing is $400/\text{XXX}/2^8$. The grid around the small black hole (m_1) starts at refinement level 11 for $q = 7$ with size $\pm 0.15625M$ and an additional grid is added for each doubling of the mass ratio with half the size, down to 18 refinement levels for q1024 with size $= \pm 0.00125M$. The minimal grid spacing is then $400/\text{XXX}/2^{(\#\text{refinement levels}-1)}$. For q1024 with resolution of n206, we would have $400/206/2^{17} = 0.000014814$ or a resolution of $M/67502$.

We are thus able to perform convergence studies at higher global resolutions than usual with reasonable amounts of computational resources and running times (for instance, for our resolution, n172, the q1024 using 18 grid refinement levels simulation took 83 days on 10 dual Intel Xeon 6242 16-core CPUs at 2.8GHz nodes, using a total of 19920 node-hours or 637440 core-hours in our white lagoon CCRG cluster).

The whole sequence of configurations studied here are described in Table I in terms of its initial parameters. The measured horizon masses follow the expected analytic Brill-Lindquist [42, 43] ratios $q = m_1/m_2 = m_1^p/m_2^p (1 + m_2^p/2R_0)/(1 + m_1^p/2R_0)$, as a function of the puncture masses m_i^p parameters in the initial data.

The extraction of gravitational radiation from the numerical relativity simulations is performed using the formulas (22) and (23) from [45] for the energy and linear momentum radiated, respectively, in terms of the ex-

tracted Weyl scalar Ψ_4 at the observer location $R_{\text{obs}} = 113M$. While in the case of the particle limit, we evolve the Zerilli equation and the waveform variable $\psi_{\ell m}$ in the time domain as in [46] and extract the energy and linear momentum as given in formulas (2) and (4) of Ref. [47]. To make a direct comparison of the numerical and perturbative results we have not removed the initial spurious radiation from either of the waveforms nor extrapolated them to infinite observer location.

SIMULATIONS' RESULTS

An important goal of this study is to assess the accuracy of our numerical methods in the so far unexplored regime of a thousand to one mass ratio black hole binaries. In order to evaluate these estimates we first perform an internal error analysis by studying the numerical convergence of gravitational radiation with resolution. Independently, the second goal is to perform an external comparison of those radiative quantities with the results of first order perturbations theory. Once we establish the accuracy of our results we can reliably start discussing potential correlations between the mode and mass ratio dependences of the non-linear (numerical relativity) approach to the linear (perturbative) regime, like our first estimate $q_{\text{linear}} \sim 1/(8\ell^2)$ below.

A technical innovation we are going to use here with respect to the previous simulations [37] is the use of a smoother gauge as given by Eq. (2) that removes the initial numerical noise. This is going to play a crucial role here, given the much lower gravitational wave amplitude levels emitted by the small mass ratio binaries studied in this paper. In particular, Eq. (2) retains the adaptivity of the gauge to the different size of the black holes on the grid, but more interestingly the asymptotic behavior of $\eta_G \rightarrow 1$ seems to much improve the extraction of gravitational radiation.

Fig. 1 represents a first display of the results of our extensive studies based on the highest resolution simulations of Table I configurations. In order to perform a direct comparison we normalize the energy by the leading dependence on the mass ratio, m_1^2/M , thus $(1+q)^2/q^2 E_{\ell m}/M$, and use their values at the extraction radius $R_{\text{obs}} = 113M$. We first note the good agreement of the computed (rescaled) radiated energy with the corresponding particle limit as we approach smaller mass ratios for all the ℓ -modes displayed here. We then note that the approach to the particle limits may depend on the value of ℓ , roughly in a sequence $q \sim 1/32, 1/64, 1/128$, and $1/256$ for $\ell = 2, 3, 4, 5$ respectively. A critical value of the mass ratio, below which the particle limit seems to be a very good approximation (within 1%) to the full numerical simulation seems to follow $q_{\text{linear}} \sim 1/(8\ell^2)$ to reach the linear regime.

Table II displays our convergence study for the total

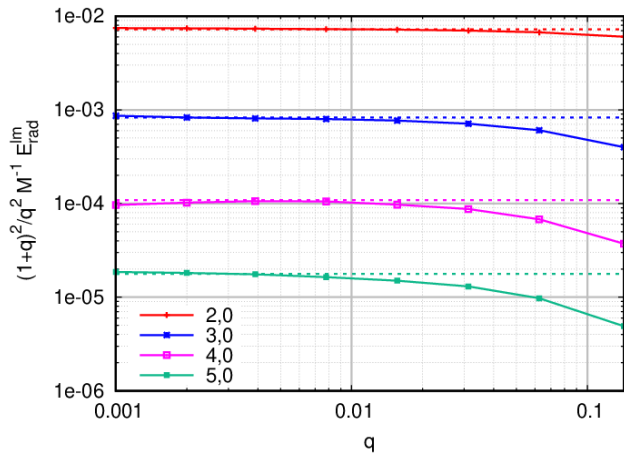


FIG. 1. Rescaled radiated energy E_{rad}/M , for each mode $\ell = 2, 3, 4, 5$ for the q7, q16, q32, q64, q128, q256, q512, q1024 simulations and the particle limit (dotted lines).

radiated energy (summed over $\ell = 2$ through $\ell = 5$) in the form of gravitational waves. We use all available runs (except those in parenthesis) at successive increasing global resolutions h (by factors of ≈ 1.2) from those labeled n084 to n206 and then use those values to fit a convergence rate γ and its value extrapolated to infinite resolution of the form $A_\infty + B h^\gamma$. The results show a high convergence rate, as expected for the 8th order spatial finite differences (with q7 being overresolved and n120 underresolving q512 and q1024), thus approaching the convergence regime, and extrapolated values close to our highest resolution available serve as an error measure. They also display very good agreement with the perturbative results in the small q cases. In fact the sequence of the radiated energy $E_{\text{rad}}^{n_\infty}$ extrapolated to infinite resolution versus q gives an approach to the particle limit that can be fitted as an expansion, $E_{\text{rad}}^{fit} = 0.00823 q^2/(1+q)^2 - 0.0315 q^3/(1+q)^3 + 0.0455 q^4/(1+q)^4$. From this expression we see that in order to be within 10% the particle limit we should be about $q < 1/32$.

A detail of the convergence versus spatial resolution dx/M of the simulation is displayed in Fig. 2 as the approach of the radiated energy to its extrapolated to infinite resolution given in Table II. We have chosen to reach resolutions that at least beat the 10^{-4} values of the rescaled quantities, i.e. a 0.1% relative error.

In a similar fashion we can study the radiation of linear momentum (in the headon collision there is no angular momentum to be radiated). In this case the coupling of modes ℓ and $\ell + 1$ in equation (4) of Ref. [47] makes the computations more sensitive and we take the opportunity to display in Fig. 3 the dependence of the results on resolution (in terms of a recoil velocity normalized by $(1+q)^2/q^2 V$ and in km/s). This is a more challenging computation since the recoil comes out as a net difference of linear momentum radiated rather than the superposi-

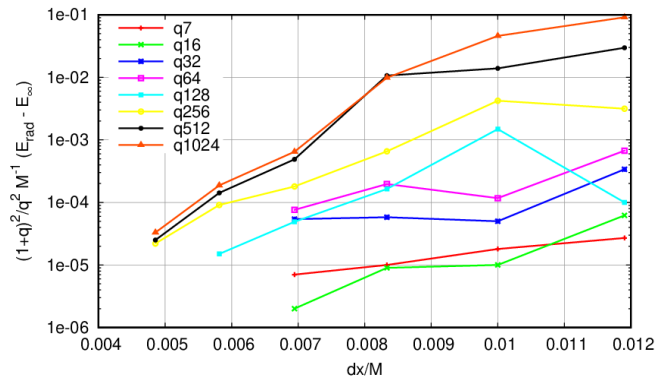


FIG. 2. Convergence study of the radiated energy to its extrapolated to infinite resolution E_∞ values in Table II for the q7, q16, q32, q64, q128, q256, q512, q1024 simulations.

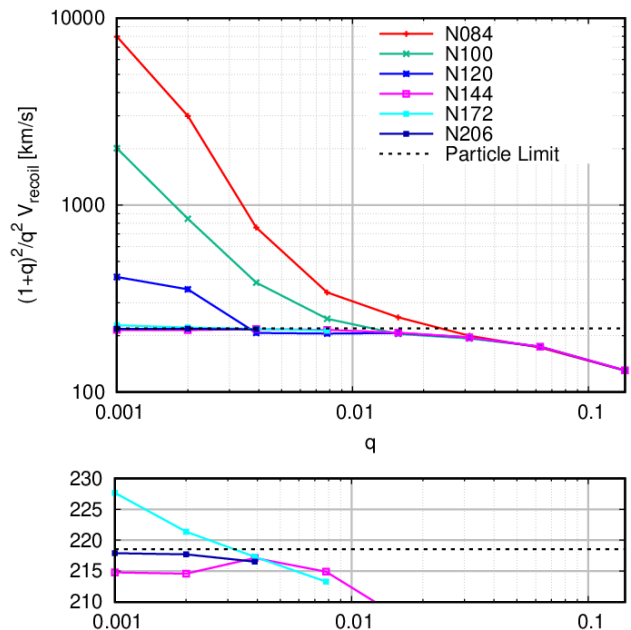


FIG. 3. Convergence study of the rescaled recoil velocity, V_{recoil} for the q7, q16, q32, q64, q128, q256, q512, q1024 simulations and the particle limit case. With a zoom-in below.

tion as in the total energy. Nevertheless the lower panel of Fig. 3 displays a notable precision with respect to the particle limit and this allows us, for instance, to assess the minimal resolution required to reliably compute linear momentum radiated. This computation of the recoil velocity thus provides us with a practical assessment of the minimal global resolution requirement in future computations at very small binary mass ratios to study the convergence regime. We will discuss this point further in the next section.

Our results are consistent with those of [24] for the 100:1 mass ratio and extrapolated to infinite observer location. Since, we extract waveforms at $R_{\text{obs}} = 113M$

TABLE II. The energy radiated, E_{rad} , summed over $\ell = 2, 3, 4, 5$ (and normalized by M/m_1^2) for each resolution of the qX simulations, starting at $D \approx 13M$ and extracted at the radius $R_{\text{obs}} = 113M$. All quantities are calculated from the gravitational waveforms. Extrapolation to infinite resolution and order of convergence is derived.

Run/resolution	n084	n100	n120	n144	n172	n206	$n\infty$	Order
q7	0.004885	0.004894	0.004902	0.004905			0.004912	2.6
q16	0.006461	0.006513	0.006514	0.006521			0.006523	8.3
q32	0.007611	0.007222	0.007330	0.007326			0.007272	8.5
q64	(0.008558)	0.008002	0.007688	0.007809			0.007885	5.5
q128	(0.008159)	(0.009545)	0.007895	0.008010	0.008044		0.008059	6.6
q256	(0.011276)	(0.012349)	(0.008778)	0.007943	0.008214	0.008145	0.008123	7.7
q512	(0.037908)	(0.022107)	(0.018858)	0.007693	0.008324	0.008207	0.008182	9.5
q1024	(0.099398)	(0.054224)	(0.018103)	0.007582	0.008416	0.008262	0.008229	9.5
qparticle							0.008230	2 [46, 48]

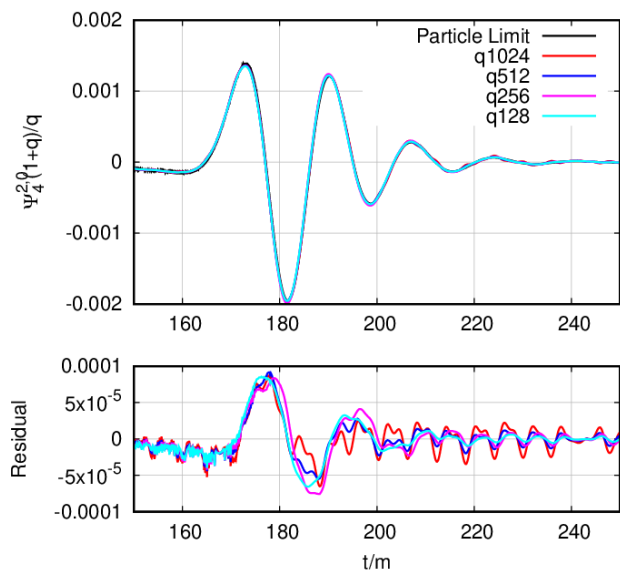


FIG. 4. Rescaled by $(1+q)/q$ waveforms Ψ_4 for the leading mode $(\ell, m) = (2, 0)$ at the observer location $R_{\text{obs}} = 113M$ for the q128, q256, q512, and q1024 simulations and the particle limit case. Bottom panel shows the differences for each mass ratio with the particle limit.

and release the smaller hole from a finite distance $R_0 = 10M$ we expect lower values for E_{rad} and V_r .

A first display of the agreement between the highest available resolution runs and the particle limit is displayed in Fig. 4. Those waveforms are rescaled by the leading dependence with the mass ratio, $(1+q)/q$, but otherwise not fitted or adjusted. The excellent superposition of waveforms shows both, the approach to the particle limit above q128, and the high accuracy of the simulations (note that the rescaling for q1024 implies a factor of nearly one thousand of amplification).

Another detailed feature of the gravitational waves is given by the spectrum of radiation (for each individual mode, in this case the leading $(\ell = 2, m = 0)$, in units

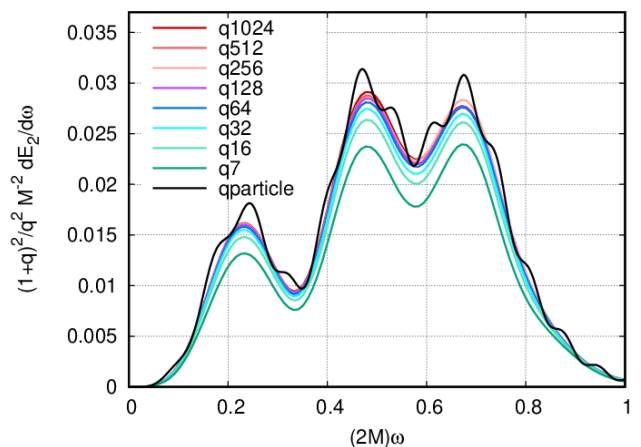


FIG. 5. Comparative scaled spectra for for the q7, q16, q32, q64, q128, q256, q512, q1024 simulations and the particle limit case.

of m_1^2) as shown in Fig. 5. This gives us the opportunity to study the approach to the linear perturbative regime. We see that for q7, q16, the spectra lies below that of the particle limit (normalized by $(1+q)^2/q^2/M^2 dE_{\ell m}/d\omega$) and only at lower values of q the spectra of the simulations approach that of the particle limit [43].

Note that the rescaling of E_ℓ and V_{recoil} by $\sim q^{-2}$ implies a precision of one in one million for the q1024 case, and errors of the order of 1% from the particle limit ensures an accuracy of the runs of 10^{-8} in this low radiation amplitude headon case.

CONCLUSIONS

Our proof of principle in this paper shows that Numerical Relativity and the moving puncture formalism can effectively be used to compute small mass ratio binaries (even 1000:1, a so far unexplored regime, and well

into the small mass ratios territory [11]) and it can accurately describe those very low amplitude gravitational waveforms. While the Zeno’s dichotomy approach [28] of adding new mesh refinement levels to describe the smaller and smaller hole proved to be appropriate to describe the sources (as monitored by the constancy of the horizon masses and spins) and the “conservative” portion of the gravitational field in the nonlinear regime, the radiative fields, that are generated at inter-black holes scales and are extracted in the asymptotic region at the observer location, scale down with the mass ratio q and eventually reach such low amplitude values that a higher global refinement of the grids is required to properly resolve them. We have thus explored the approach to the convergence regime and have seen that using the radiated energy as a reference, the simulations with resolution n084 are sufficient to approximate results for the up to q16 while the q64 requires at least n100, q256 requires at least n120, and so on until we reached q1024, requiring at least n144. This gives a rule-of-thumb for the minimal resolution h_{min} from a base resolution $h_0 = 0.84$ to solve accurately a mass ratio binary as small as $q \approx \frac{1}{16}(h_0/h_{min})^8$. We confirmed the results with n172 resolution runs (globally doubling that of n084) as shown in Table II. At further higher resolutions one may then consider dropping one of the innermost refinement levels to make simulations more efficient.

We have found that the gauge η_G in (2) notably improves the numerical noise from our previous $\eta(W)$ used in [23]. We also found that the $\eta = 1$ gauge works similarly well, suggesting that the lower asymptotic values of η allow for a smooth and accurate transport of radiation from the sources to the extraction regions [37, 49], and that the benefits of an adapted gauge around the horizons is somewhat taken care of by the additional refinement levels required to resolve the small hole. The choice of gauge and the appropriate minimal global resolutions that warrant the convergence regime providing valuable quantitative results for the radiation, orbital trajectories, and remnant of the very small mass ratio binary black hole mergers, will help us establishing initial parameters for further orbital evolutions studies.

We have also established for what values of q , linear theory begins to work (or break down) in a merger regime. We have been able to make a first rough estimate for the threshold value $q_{linear} \leq 1/(8\ell^2)$ dependence on the ℓ -mode. This deserves further study, including higher modes and accuracy, in the orbital case. Mode decomposition is often used in the phenomenological modeling of gravitational waves and in self-force calculations which include much higher ℓ -modes [19]. Higher ℓ -modes not only are smaller in amplitude but of higher frequency content, leading not only to resolution issues but also to resilience of nonlinearities (involving derivatives of the fields), as we can infer from our study.

Finally, we note that since the current numerical rel-

ativity codes display a good constant load (weak) scaling, with larger computational resources they can deal with an increase in resolution of the current simulations, and perform explorations of the binary’s parameter space (with the advantage of having to deal with increased amplitude of the gravitational radiation) that may include precession and the spin of the large hole at essentially no extra delays from the base case that used $\mathcal{O}(10)$ computer nodes per run [28]. Much longer numerical evolutions in time (scaling like $\mathcal{O}(1/q)$), in the intermediate to small mass ratio regime, would benefit of any future software and hardware speedups by the time of 3G detectors operation and LISA launch, but our use of a low Courant factor (1/4) warrants to keep the accuracy of those long term merger simulations and they could be coupled with a hybridization of the waveform when the binary is at larger initial separations than those considered in our pure numerical simulations. Further work will be needed in order to determine precisely what advances will be necessary for binary-black-hole simulations with mass ratios of 1000:1 to achieve sufficient accuracy (at a feasible cost) for application to LISA and 3G gravitational-wave detectors.

The authors gratefully acknowledge the National Science Foundation (NSF) for financial support from Grants No. PHY-1912632 and PHY-2207920. Computational resources were also provided by the New Horizons, Blue Sky, Green Prairies, and White Lagoon clusters at the CCRG-Rochester Institute of Technology, which were supported by NSF grants No. PHY-0722703, No. DMS-0820923, No. AST-1028087, No. PHY-1229173, No. PHY-1726215, and No. PHY-2018420. This work used the Extreme Science and Engineering Discovery Environment (XSEDE) [allocation TG-PHY060027N], which is supported by NSF grant No. ACI-1548562 and project PHY20007 Frontera, an NSF-funded Petascale computing system at the Texas Advanced Computing Center (TACC). The authors also thank the referees of this work for numerous useful suggestions on how to improve the presentation of results.

-
- [1] B. P. Abbott *et al.* (LIGO Scientific, Virgo), *Phys. Rev. Lett.* **116**, 061102 (2016), arXiv:1602.03837 [gr-qc].
 - [2] R. Abbott *et al.* (LIGO Scientific, VIRGO, KAGRA), (2021), arXiv:2111.03606 [gr-qc].
 - [3] M. Campanelli, C. O. Lousto, P. Marronetti, and Y. Zlochower, *Phys. Rev. Lett.* **96**, 111101 (2006), gr-qc/0511048.
 - [4] G. Lovelace *et al.*, *Class. Quant. Grav.* **33**, 244002 (2016), arXiv:1607.05377 [gr-qc].
 - [5] J. Healy and C. O. Lousto, *Phys. Rev. D* **102**, 104018 (2020), arXiv:2007.07910 [gr-qc].
 - [6] J. Healy, C. O. Lousto, J. Lange, and R. O’Shaughnessy, *Phys. Rev. D* **102**, 124053 (2020), arXiv:2010.00108 [gr-qc].

- [7] J. R. Gair, S. Babak, A. Sesana, P. Amaro-Seoane, E. Barausse, C. P. Berry, E. Berti, and C. Sopuerta, *J. Phys. Conf. Ser.* **840**, 012021 (2017), arXiv:1704.00009 [astro-ph.GA].
- [8] M. Pürrer and C.-J. Haster, *Phys. Rev. Res.* **2**, 023151 (2020), arXiv:1912.10055 [gr-qc].
- [9] M. Maggiore *et al.*, *JCAP* **03**, 050 (2020), arXiv:1912.02622 [astro-ph.CO].
- [10] D. Reitze *et al.*, *Bull. Am. Astron. Soc.* **51**, 035 (2019), arXiv:1907.04833 [astro-ph.IM].
- [11] P. Amaro-Seoane *et al.*, (2022), arXiv:2203.06016 [gr-qc].
- [12] T. Regge and J. A. Wheeler, *Phys. Rev.* **108**, 1063 (1957).
- [13] F. J. Zerilli, *Phys. Rev. D* **2**, 2141 (1970).
- [14] S. A. Teukolsky, *Astrophys. J.* **185**, 635 (1973).
- [15] Y. Mino, M. Sasaki, and T. Tanaka, *Phys. Rev.* **D55**, 3457 (1997), arXiv:gr-qc/9606018.
- [16] T. C. Quinn and R. M. Wald, *Phys. Rev.* **D56**, 3381 (1997), arXiv:gr-qc/9610053.
- [17] C. O. Lousto, *Phys. Rev. Lett.* **84**, 5251 (2000), gr-qc/9912017.
- [18] L. Barack and C. O. Lousto, *Phys. Rev. D* **66**, 061502 (2002), gr-qc/0205043.
- [19] L. Barack and A. Pound, *Rept. Prog. Phys.* **82**, 016904 (2019), arXiv:1805.10385 [gr-qc].
- [20] Y. Pan *et al.*, *Phys. Rev.* **D81**, 084041 (2010), arXiv:0912.3466 [gr-qc].
- [21] S. Khan, S. Husa, M. Hannam, F. Ohme, M. Pürrer, X. Jiménez Forteza, and A. Bohé, *Phys. Rev.* **D93**, 044007 (2016), arXiv:1508.07253 [gr-qc].
- [22] J. Blackman, S. E. Field, M. A. Scheel, C. R. Galle, C. D. Ott, M. Boyle, L. E. Kidder, H. P. Pfeiffer, and B. SzilA!gyi, *Phys. Rev.* **D96**, 024058 (2017), arXiv:1705.07089 [gr-qc].
- [23] C. O. Lousto and Y. Zlochower, *Phys. Rev. Lett.* **106**, 041101 (2011), arXiv:1009.0292 [gr-qc].
- [24] U. Sperhake, V. Cardoso, C. D. Ott, E. Schnetter, and H. Witek, *Phys. Rev.* **D84**, 084038 (2011), arXiv:1105.5391 [gr-qc].
- [25] W. G. Cook, U. Sperhake, E. Berti, and V. Cardoso, *Phys. Rev. D* **96**, 124006 (2017), arXiv:1709.10514 [gr-qc].
- [26] S. Husa, S. Khan, M. Hannam, M. Pürrer, F. Ohme, X. Jiménez Forteza, and A. Bohé, *Phys. Rev.* **D93**, 044006 (2016), arXiv:1508.07250 [gr-qc].
- [27] J. Yoo, V. Varma, M. Giesler, M. A. Scheel, C.-J. Haster, H. P. Pfeiffer, L. E. Kidder, and M. Boyle, *Phys. Rev. D* **106**, 044001 (2022), arXiv:2203.10109 [gr-qc].
- [28] C. O. Lousto and J. Healy, *Phys. Rev. Lett.* **125**, 191102 (2020), arXiv:2006.04818 [gr-qc].
- [29] A. Nagar, J. Healy, C. O. Lousto, S. Bernuzzi, and A. Albertini, (2022), arXiv:2202.05643 [gr-qc].
- [30] Y. Zlochower, J. G. Baker, M. Campanelli, and C. O. Lousto, *Phys. Rev.* **D72**, 024021 (2005), arXiv:gr-qc/0505055.
- [31] C. O. Lousto and Y. Zlochower, *Phys. Rev.* **D77**, 024034 (2008), arXiv:0711.1165 [gr-qc].
- [32] C. O. Lousto and J. Healy, *Phys. Rev.* **D99**, 064023 (2019), arXiv:1805.08127 [gr-qc].
- [33] J. Healy, C. O. Lousto, and Y. Zlochower, *Phys. Rev.* **D90**, 104004 (2014), arXiv:1406.7295 [gr-qc].
- [34] J. Healy and C. O. Lousto, *Phys. Rev.* **D95**, 024037 (2017), arXiv:1610.09713 [gr-qc].
- [35] J. Healy, C. O. Lousto, and Y. Zlochower, *Phys. Rev.* **D96**, 024031 (2017), arXiv:1705.07034 [gr-qc].
- [36] J. Healy *et al.*, *Phys. Rev.* **D97**, 064027 (2018), arXiv:1712.05836 [gr-qc].
- [37] N. Rosato, J. Healy, and C. O. Lousto, *Phys. Rev. D* **103**, 104068 (2021), arXiv:2103.09326 [gr-qc].
- [38] Y. Zlochower, M. Ponce, and C. O. Lousto, *Phys. Rev.* **D86**, 104056 (2012), arXiv:1208.5494 [gr-qc].
- [39] J. Healy, C. O. Lousto, Y. Zlochower, and M. Campanelli, *Class. Quant. Grav.* **34**, 224001 (2017), arXiv:1703.03423 [gr-qc].
- [40] J. Healy, C. O. Lousto, J. Lange, R. O’Shaughnessy, Y. Zlochower, and M. Campanelli, *Phys. Rev.* **D100**, 024021 (2019), arXiv:1901.02553 [gr-qc].
- [41] J. Healy and C. O. Lousto, *Phys. Rev. D* **105**, 124010 (2022), arXiv:2202.00018 [gr-qc].
- [42] D. Brill and R. Lindquist, *Phys. Rev.* **131**, 471 (1963).
- [43] C. O. Lousto and R. H. Price, *Phys. Rev. D* **55**, 2124 (1997), gr-qc/9609012.
- [44] C. O. Lousto and Y. Zlochower, *Phys. Rev.* **D88**, 024001 (2013), arXiv:1304.3937 [gr-qc].
- [45] M. Campanelli and C. O. Lousto, *Phys. Rev.* **D59**, 124022 (1999), arXiv:gr-qc/9811019 [gr-qc].
- [46] C. O. Lousto and R. H. Price, *Phys. Rev. D* **56**, 6439 (1997), gr-qc/9705071.
- [47] C. O. Lousto and R. H. Price, *Phys. Rev.* **D69**, 087503 (2004), gr-qc/0401045.
- [48] C. O. Lousto, *Class. Quant. Grav.* **22**, S543 (2005), gr-qc/0503001.
- [49] J. Healy, C. O. Lousto, and N. Rosato, *Phys. Rev. D* **102**, 024040 (2020), arXiv:2003.02286 [gr-qc].